mediately in the reverse reaction, oxidation of a small fraction by the disulfide bonds, eq 7, and other oxidants such as O_2 will

$$PEt_3 + RSSR + H_2O \rightarrow 2RSH + Et_3PO \quad (7)$$

gradually shift the equilibrium to the right. Although the net equilibrium of the first step should lie far to the left, the second reaction is irreversible and drives the overall process to completion.

In previous studies of reactions between $[(Et_3P)_2Au]Cl$ and small organic disulfides, the apparent rate-limiting step was dissociation of a phosphine ligand from gold.[12] A similar mechanism apparently operates in the case of the sulfhydryl modified albumins. They initially lack any free sulfhydryls and can not react according to eq 6 and 7. The observation that they do react with $[(Et_3P)_2Au^+]$, although more slowly than does AlbSH, can be explained by eq 8-10. If this sequence were the

$$[(Et_3P)_2Au]Cl \rightleftarrows Et_3PAuCl + Et_3P \quad (8)$$

$$Et_3P + \overset{\frown}{S_2}BSA \xrightarrow{H_2O} (HS)_2BSA + Et_3PO \quad (9)$$

$$Et_3PAuCl + (HS)_2BSA \rightarrow (Et_3PAuS)_x(SH)_{2-x}BSA + H^+ + Cl^- \quad (10)$$

dominant mechanism, the reactions of the modified and unmodified albumins (Cy-BSA and Ac-BSA vs AlbSH) should occur at similar rates. The delay observed with Ac-BSA, in particular (compare Figure 1b and Figure 2a), is consistent with eq 8-10. It further suggests an important role for Cys-34 in the rate-determining step of the AlbSH reaction, as indicated in eq 6.

$[(Et_3P)_2Au]Cl$ differs from auranofin ($Et_3PAuSAtg$) in the physical and chemical properties that might affect its molecular pharmacology. For example, the bis(phosphine) complex is moderately soluble in aqueous solution, while auranofin is only sparingly soluble. Excess $[(Et_3P)_2Au]Cl$ denatures serum albumin,[9] but auranofin does not.[5,9,10] Nonetheless, $[(Et_3P)_2Au]Cl$ generates $AlbSAuPEt_3$ and Et_3PO as the dominant products when it reacts with equimolar or excess albumin (Figure 1b). These are the same products formed in albumin-auranofin reactions.[5] Although the bis(phosphine) complex generates Et_3PO more rapidly and more extensively than auranofin and also forms $(Et_3PAuS)_x(SH)_{2-x}BSA$ as a likely metabolite, the oxide is not medicinally significant and the gold bound to the newly generated, low-affinity cysteines should be at least as active as Cys-34-bound gold. Thus, it is not surprising that $[(Et_3P)_2Au]Cl$ and auranofin have similar activities in the adjuvant-induced arthritic rat assay (Table II).

Elucidation of the sulfur chemistry of serum albumin has been hampered by a lack of suitably sensitive and specific spectroscopic probes. For example, the NMR signals of sulfur-33, the only NMR-active isotope, are too broad to be used for most purposes. We have demonstrated here that Cys-34 and any nonnative cysteines generated by reduction of the internal disulfide bonds can be distinguished by ^{31}P NMR after titration with Et_3PAu^+. This finding provides a new tool for exploring the chemistry of Cys-34 and the internal and external disulfides bonds.

Abbreviations: AAS, atomic absorption spectroscopy; Ac-BSA, BSA modified to convert AlbSH to $AlbSCH_2CONH_2$; AlbSH, mercaptalbumin (a BSA component); AlbSSCy, the cysteine disulfide of albumin Cys-34; AlbSSGt, the glutathione disulfide of albumin Cys-34; BSA, microheterogeneous bovine serum albumin; Cy-BSA; BSA modified to convert AlbSH to AlbSSCy; DTNB, 5,5'-dithiobis(2-nitrobenzoic acid); GC-MS, gas chromatography-mass spectroscopy; $(HS)_2BSA$, albumin-containing reduced disulfide bonds; NMR, nuclear magnetic resonance; ppm, parts per million; TMP, trimethyl phosphate.

Registry No. I, 65583-79-1; Et_3P, 554-70-1.

Contribution from the Department of Chemistry,
Dartmouth College, Hanover, New Hampshire 03755

Magnetic Properties of the Nickel Enzymes Urease, Nickel-Substituted Carboxypeptidase A, and Nickel-Substituted Carbonic Anhydrase

Patrick A. Clark and Dean E. Wilcox*

Received July 22, 1987

Magnetic susceptibility measurements have been made on urease and the Ni-substituted forms of carboxypeptidase A (Ni-CPA) and carbonic anhydrase (Ni-CA). The effective magnetic moment per Ni ion in each protein is found to be in the range consistent with six-coordinate Ni(II). Each Ni-protein exhibits low-temperature deviations from the Curie law behavior, and for Ni-CPA and Ni-CA this correlates with axial zero-field splittings the $^3A_2$ ground state of 3.5 and -8.2 cm^{-1}, respectively. The significantly larger magnitude of this deviation observed for urease indicates a magnetic interaction between the two Ni(II) ions in each subunit. Fitting the urease magnetic data indicates a weak antiferromagnetic exchange coupling of the Ni(II) ions ($J = -6.3$ cm^{-1}, using the isotropic exchange Hamiltonian $H = -2JS_1 \cdot S_2$) and an axial zero-field splitting ($D = -6.9$ cm^{-1}) consistent with distorted six-coordinate ligation of the two Ni(II) ions; this experimentally demonstrates for the first time that *urease has a binuclear Ni active site*. A magnetic contribution of single Ni(II) ions, which corresponds to ~20% of the urease Ni, is required for this fit and may be associated with a small heterogeneous subset of sites. The potent competitive inhibitor acetohydroxamic acid increases the urease magnetic moment, indicating a change in the Ni(II) coordination number and/or geometry, and diminishes the low-temperature Curie law deviation, indicating a decrease in the Ni-Ni interaction. Binding of the competitive inhibitor 2-mercaptoethanol (2-ME) results in a diamagnetic Ni(II) ground state for ~80% of the urease Ni ions. The residual moment of this derivative appears to correlate with a percentage of sites where 2-ME apparently does not bind or binds differently than in the dominant ~80% of active sites; this subset of paramagnetic sites may correlate with the native urease sites lacking binuclear interaction. In contrast to urease, 2-ME binding to Ni-CA does not reduce the paramagnetism of the active site Ni(II) ion, suggesting a unique Ni-thiolate interaction for urease. The ligand field absorption spectrum of 2-ME-bound urease does not show intense orbitally allowed transitions associated with a low-spin $^1A_1$ Ni(II) ground state, indicating that the diamagnetism of this inhibitor-bound form appears to be due to a stronger antiferromagnetic exchange interaction between the Ni(II) ions; this further supports a binuclear active site in urease and suggests the possibility of bridging coordination for substrates.

Introduction

Urease (EC 3.5.1.5) catalyses the hydrolysis of urea and was the first enzyme recognized[1] to contain and require Ni for catalytic activity. The enzyme isolated from jack bean has two Ni ions per 96 600-Da subunit and is aggregated into a hexamer of subunits. Urease will hydrolyze a limited number of substrates[2] other

* To whom correspondence should be addressed.

(1) Dixon, N. E.; Gazzola, C.; Blakeley, R. L.; Zerner, B. *J. Am. Chem. Soc.* **1975**, *97*, 4130-4133.

0020-1669/89/1328-1326$01.50/0

than urea, and several competitive inhibitors of the enzyme are known.

While the protein properties of urease have recently become better characterized, little is known about the structural and electronic properties of the active-site nickel ion(s). Weak absorption features in the visible and near-IR regions have been correlated[3] with the d–d transitions of six-coordinate $\sim O_h$ Ni(II) ions. However, the reported ligand field absorption spectrum[3] and the associated CD spectrum[4] of urease both have features in addition to the three expected spin-allowed transitions of O_h Ni(II). A Ni EXAFS study[5] of urease has indicated that the coordination of the Ni ions includes five or six ligands with N and O donor atoms; the lack of first-shell S ligands in native urease has been confirmed in a recent Ni X-ray absorption study.[6]

Ni(II) can be successfully substituted for the Zn(II) ion in certain Zn-containing enzymes, such as carboxypeptidase A (CPA)[7] and carbonic anhydrase (CA).[8] These two are of interest for comparison to urease because of the similarity of their hydrolytic reactions to that of urease and the apparent absence of S donor ligands for the active-site metal ion. Ni-CPA is particularly worthy because it retains significant amounts of both peptidase and esterase activity and its crystal structure has been determined;[9] the crystallized protein form has a square-pyramidal Ni coordination. This geometry, however, is in disagreement with the results of an earlier spectroscopic study of Ni-CPA that indicated[10] $\sim O_h$ Ni(II) coordination. The ligands and coordination geometry of Ni-CA are not known; however, weak ligand field transitions suggest[11] a six-coordinate Ni(II) geometry near neutral pH. An increase in the intensity of these transitions at higher pH has been interpreted[11] as a change in the Ni(II) coordination.

In order to understand the urease catalytic mechanism, the factors leading to its remarkable $\sim 10^{14}$ rate enhancement of urea hydrolysis, and the basis for the required Ni ions in this enzyme, it is necessary to characterize the properties of the urease Ni ions and their role in the catalytic mechanism. We have begun such studies using a variety of physical and spectroscopic methods to provide new insight about the urease active site and interaction of the Ni ions with substrates and inhibitors. While each urease subunit contains two Ni ions and one active site,[1] there is currently no evidence for a binuclear Ni active site in urease. In order to evaluate the possibility of Ni–Ni interaction, we are correlating our results on urease with analogous results on the mononuclear enzymes Ni-CPA and Ni-CA and will be extending these studies to include relevant small molecule Ni(II) complexes. Our initial study has involved characterization of the ground-state magnetic properties of these three nickel enzymes.

The magnetic properties of Ni(II) provide[12] a valuable probe of its coordination geometry and electronic structure. Deviation of the Ni(II) magnetic moment from the $S = 1$ spin-only value of $\mu_{eff} = 2.83\ \mu_B$ is due to spin–orbit coupling and therefore reflects the coordination geometry[13] of the ion. Spin–orbit coupling can also result in axial (D) and rhombic (E) zero-field splitting of the Ni(II) triplet ground state. These perturbations lift the ground-state spin degeneracy in the absence of a magnetic field and, under conditions of low temperature and high magnetic field, result in a measured susceptibility lower than that expected from the Curie law.[14] For six-coordinate Ni(II) the magnitude of this effect is typically $|D| < 10\ cm^{-1}$, with $E < D/3$. In addition, exchange interaction between paramagnetic ions also results in deviations from the Curie law behavior, with antiferromagnetic coupling leading to deviations qualitatively similar to that of zero-field splitting. Thus, a detailed analysis of the magnetic properties of Ni(II) can provide an important insight about its coordination in biological systems.

Experimental Section

Urease was isolated from jack bean meal (Pacchem Laboratories, Albany, OR) by the method of Blakeley et al.[15] with omission of the chloroform–acetone defatting step; lack of this step reduces the initial yield by ~50% but does not affect the final purity. Isolated urease was further purified to near the maximum reported specific activity (~2700 IU/mg) by thiol–disulfide exchange chromatography on a glutathione-derivatized Sephrose column.[16] Further purification to remove higher molecular weight aggregates was accomplished with anaerobic gel-permeation chromatography on a Sephacryl S-300 column. Urease activity, defined by the international unit (IU) as the amount of urease capable of liberating 1 μmol of ammonia from urea/min at 25 °C and pH 7.0, was determined by Nesslerization assay.[17] A 20 mM phosphate, 1 mM EDTA, and pH 7.0 buffer was used for magnetic susceptibility measurements on urease; protein concentration was determined by using the 280-nm molar extinction value per subunit of 62000 $M^{-1}\ cm^{-1}$.[18]

Ni-substituted carbonic anhydrase was prepared from bovine erythrocyte carbonic anhydrase obtained from Sigma Chemical Co. (90% B isozyme[19]) and was used without further purification. Removal of the Zn(II) was accomplished by the method of Hunt et al.;[20] success was determined by loss of esterase activity relative to the native enzyme using 1 mM *p*-nitrophenyl acetate (Sigma) as the substrate in 0.01 M diethyl malonate buffer at 25 °C and pH 7.0.[21] Ni reconstitution involved incubation of the apoenzyme with a slightly substoichiometric concentration of $NiSO_4$ for 24 h at 4 °C; the resulting sample had nearly 1 mol equiv of Ni bound to the protein. A 0.1 M Tris, 1.0 M NaCl, and pH 7.0 (25 °C; frozen solution pH ~7.8) buffer was used for magnetic susceptibility measurements on Ni-CA; protein concentration was determined by using the 280-nm molar extinction value of 57000 $M^{-1}\ cm^{-1}$.[20]

Ni-substituted carboxypeptidase A was prepared from bovine pancrease carboxypeptidase A obtained from Sigma Chemical Co. (type 1 prepared by the method of Cox et al.[22]); dialysis against 0.10 M Tris, 1.0 M NaCl, and pH 7.0 buffer removed toluene in the aqueous suspension before further procedures. The apo protein was prepared by the method of Vallee et al.[23] with success verified by loss of peptidase activity relative

(2) Dixon, N. E.; Riddles, P. W.; Gazzola, C.; Blakeley, R. L.; Zerner, B. *Can. J. Biochem.* **1980**, *59*, 1335–1344.
(3) Blakeley, R. L.; Dixon, N. E.; Zerner, B. *Biochim. Biophys. Acta* **1983**, *744*, 219–229.
(4) Clark, P. A.; Wilcox, D. E. To be submitted for publication.
(5) Hasnain, S. S.; Piggott, B. *Biochem. Biophys. Res. Commun.* **1983**, *112*, 279–283.
(6) Clark, P. A.; Wilcox, D. E.; Scott, R. A. *Inorg. Chem.*, submitted for publication.
(7) Coleman, J. E.; Vallee, B. L. *J. Biol. Chem.* **1960**, *235*, 390–395.
(8) Coleman, J. E. *Nature* **1967**, *214*, 193–194.
(9) Hardman, K. D.; Lipscomb, W. N. *J. Am. Chem. Soc.* **1984**, *106*, 463–464.
(10) Rosenberg, R. C.; Root, C. A.; Gray, H. B. *J. Am. Chem. Soc.* **1975**, *97*, 21–26.
(11) (a) Bertini, I.; Borghi, E.; Luchinat, C. *Bioinorg. Chem.* **1978**, *9*, 495–504. (b) Bertini, I.; Borghi, E.; Luchinat, C.; Monnanni, R. *Inorg. Chim. Acta* **1982**, *67*, 99–102.
(12) (a) Figgis, B. N.; Lewis, J. In *Progress in Inorganic Chemistry*; Cotton, F. A., Ed.; Interscience: New York, 1964; Vol. 6, pp 37–239. (b) Sacconi, L. In *Transition Metal Chemistry*; Carlin, R. L., Ed.; Dekker: Berlin, 1968; Vol. 4, pp 199–298.
(13) Octahedral Ni(II) has a $^3A_{2g}$ ground state, and six-coordinate Ni(II) complexes have magnetic moments typically in the range 2.9–3.2 μ_B. Paramagnetic square-pyramidal and trigonal-bipyramidal Ni(II) complexes have magnetic moments in the range 3.2–3.4 μ_B. Tetrahedral Ni(II) has a $^3T_1$ ground state and a room-temperature moment near 4.0 μ_B that drops with lower temperature; small deviations from T_d symmetry will lower this moment typically into the range 3.5–3.9 μ_B, while large deviations lead to even lower moments. Square-planar Ni(II) complexes are diamagnetic, but at some point on the four-coordinate D_{2d} distortion pathway from D_{4h} to T_d, the ground state will change from a spin singlet (diamagnetic) to a spin triplet (paramagnetic).
(14) (a) Carlin, R. L. *Magnetochemistry*, 2nd ed.; Springer-Verlag: Berlin, 1986. (b) White, R. M. *Quantum Theory of Magnetism*, 2nd ed.; Springer-Verlag: Berlin, 1983.
(15) Blakeley, R. L.; Webb, E. C.; Zerner, B. *Biochemistry* **1969**, *8*, 1984–1990.
(16) Brocklehurst, K.; Carlsson, J.; Kierstan, M. P. J.; Crook, E. M. *Methods Enzymol.* **1974**, *34B*, 531–544.
(17) Carlsson, J.; Axen, R.; Brocklehurst, K.; Crook, E. M. *Eur. J. Biochem.* **1974**, *44*, 189–194.
(18) Dixon, N. E.; Hinds, J. A.; Fihelly, A. K.; Gazzola, C.; Winzor, D. L.; Blakeley, R. L.; Zerner, B. *Can. J. Biochem.* **1980**, *58*, 1323–1334.
(19) Personal communication to J. D. Goldman from the Technical Department, Sigma Chemical Co.
(20) Hunt, J. B.; Rhee, M.-J.; Storm, C. B. *Anal. Biochem.* **1977**, *79*, 614–617.
(21) Verpoorte, J. A.; Mehta, S.; Edsall, J. T. *J. Biol. Chem.* **1967**, *242*, 4221–4229.
(22) Cox, D. J.; Bovard, F. C.; Bargetzi, J.-P.; Walsh, K. A.; Neurath, H. *Biochemistry* **1964**, *3*, 44–47.

to the native enzyme obtained by using *N*-carbobenzoxyglycyl-L-phenylalanine (Sigma) as the substrate in the pH 7.0 buffer at 25 °C.[24] Ni substitution involved incubation for 24 h at 4 °C with a stoichiometric amount of $NiSO_4$ followed by extensive dialysis to remove loosely bound Ni(II); the resulting sample had 0.44 mol equiv of Ni bound to the protein. Peptidase activity of Ni-CPA was measured relative to the native enzyme as indicated above. Magnetic susceptibility measurements on Ni-CPA were obtained by using the same buffer as for Ni-CA; protein concentration was determined by using the 278-nm molar extinction value of 64 200 M^{-1} cm^{-1}.[25]

Metal contamination during metal substitution procedures was avoided by using deionized water, buffer solutions passed through a Chelex 100 column, and plasticware washed with 1.0 mM EDTA solution; ultrapure $NiSO_4$, NaOH, HNO_3, and HCl reagents (Johnson Matthey) were used throughout. Ni concentration in all protein samples was determined with a Perkin-Elmer 503 atomic absorption spectrometer equipped with a HGA-2100 graphite furnace.

Variable-temperature magnetic susceptibility measurements at 50 kG (2–240 K) and 10 kG (6.5–200 K) were made on a SHE Model 905 SQUID magnetometer at the Francis Bitter National Magnet Laboratory, MIT; preliminary measurements were made on a similar instrument at USC. A Delrin bucket was filled with the Ni protein samples (120–150 μL, 1.5–3.5 mM in Ni), securely capped, and suspended in the magnetometer antechamber by a cotton thread. The antechamber was then flushed with He gas for ~2 min to remove oxygen before loading the sample into the cold magnetometer; magnetic anomalies[26] at 40 K due to the antiferromagnetic transition of condensed O_2 were not observed for any sample. Separate susceptibility measurements under identical conditions were made on the buffer solution to subtract bucket, buffer, and dissolved oxygen contributions from the measured susceptibility.

To check for the possibility of magnetic noise[26] due to slowly relaxing $I = {}^1/_2$ nuclei of water and the Delrin bucket, separate sets of measurements were taken on native urease, AHA-bound urease, 2-ME-bound urease, and Ni-CA samples in deuterated 20 mM phosphate buffer ($pH^*_{uncor} = 6.8$) and suspended in a Suprasil quartz bucket etched in 10% HF to remove surface paramagnetic impurities. After brief flushing of the SQUID antechamber with He gas, the sample was rapidly loaded into the cold magnetometer to freeze the sample and minimize evaporative loss. Effective moments obtained under these conditions were found to be within experimental error of the earlier measurements in proton-containing buffer and the Delrin bucket.

Each susceptibility measurement at a given temperature has been converted to molar susceptibility (χ_m) per Ni ion by using the weight, density, and Ni concentration of the sample. Plots of the molar susceptibility per Ni ion vs $1/T$ have been rescaled to pass through zero at infinite temperature, thus subtracting the protein diamagnetism and Ni(II) temperature-independent paramagnetism. The effective magnetic moment (μ_{eff}) in units of Bohr magnetons (μ_B) was obtained from the slope of these plots in the high-temperature region where the data obeys the Curie law, $\chi_m = C/T = N\mu_{eff}^2/3kT$, where C, N, and k are the Curie, Avogadro, and Boltzmann constants, respectively.

Urease absorption spectra were obtained at ambient temperature on a Perkin-Elmer λ-9 spectrometer using matched 1.00 cm path length cells and on a Cary 14 spectrometer using matched 5.00 cm path length cells. Light scattering by the large protein hexamer was subtracted as described in ref 3.

Results

The magnetic susceptibility of urease, Ni-CPA and Ni-CA have been determined over the temperature range 6–240 K. While the temperature-independent protein diamagnetism makes the largest contribution to the observed susceptibility, the Ni(II) paramagnetism contributes the temperature-dependent component of the susceptibility. The χ_m vs $1/T$ plots of this temperature-dependent component for these three nickel enzymes are shown in Figure 1. At higher temperatures ($T > 60$ K for urease; $T > 30$ K for Ni-CA and Ni-CPA) all three data sets follow a linear Curie law behavior and the effective magnetic moment (μ_{eff}) per Ni ion can be determined.

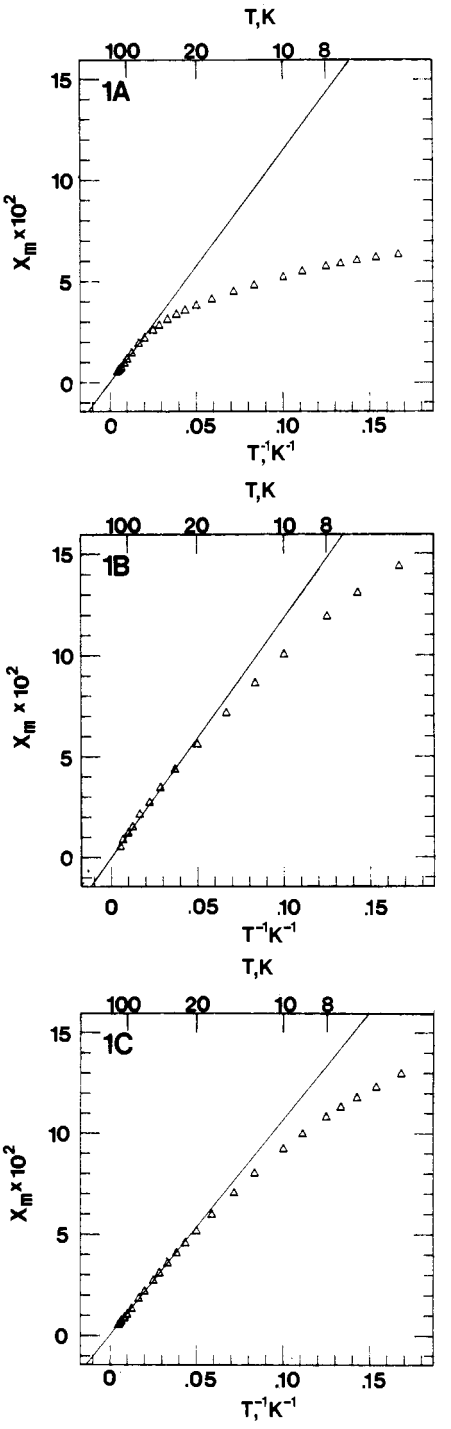

Figure 1. Plot of the 50-kG molar susceptibility per Ni ion vs $1/T$ for (A) urease (pH 7.0), (B) Ni-CPA (pH ~7.8), and (C) Ni-CA (pH ~7.8). Solid lines are best linear fits for the $T \geq 60$ K urease data and the $T \geq 30$ K Ni-CPA and Ni-CA data.

For urease (Figure 1A) we obtain an effective magnetic moment per Ni(II) ion of 3.04 ± 0.10 μ_B, which is a value typical of ~O_h-coordinated Ni(II) and establishes a $^3A_2$ ground state. This is an average effective moment for the two ions in each subunit and indicates that both are paramagnetic. If the effective moment of each Ni(II) ion is assumed to be greater than or equal to the spin-only value, then each urease Ni(II) ion has an effective moment in the range $2.83 < \mu_{eff} < 3.25$ μ_B; this, in conjunction with electronic spectral data (vide infra), indicates that both ions are six-coordinate. Figure 1A shows that a significant deviation from the Curie law behavior is observed at low temperature for urease.

The magnetic susceptibility of Ni-CPA has been measured previously, and an effetive magnetic moment of 2.53 ± 0.10 μ_B was reported.[27] Prompted in part by this low μ_{eff} value and the

(23) Vallee, B. L.; Rupley, J. A.; Coombs, T. L.; Neurath, H. *J. Biol. Chem.* **1960**, *235*, 64–69.
(24) Billo, E. J.; Brito, K. K.; Wilkins, R. G. *Bioinorg. Chem.* **1978**, *8*, 461–475.
(25) Simpson, R. T.; Riordan, J. F.; Vallee, B. L. *Biochemistry* **1963**, *2*, 616–622.
(26) Day, E. P.; Kent, T. A.; Lindahl, P. A.; Munck, E.; Orme-Johnson, W. H.; Roder, H.; Roy, H. *Biophys. J.* **1987**, *52*, 837–853.

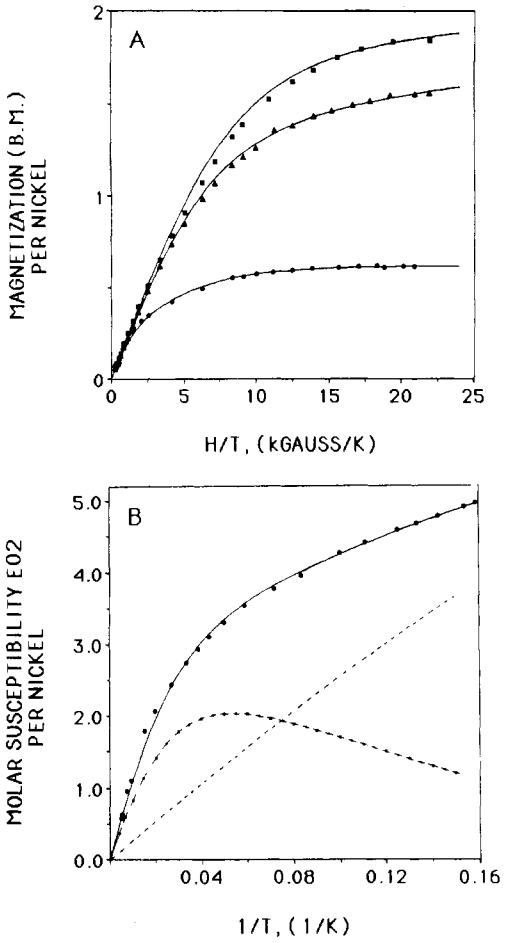

Figure 2. (A) 50-kG magnetization data for Ni-CPA (■) pH ~7.8, Ni-CA (▲) pH ~7.8, and urease (●) pH 7.0. Solid lines are best fits to the data for Ni-CPA and Ni-CA using a single-ion spin Hamiltonian and fit parameters indicated in the text and for urease using a weighted combination of a spin Hamiltonian including isotropic exchange and a $S = 1$ Brillouin function and the fit parameters indicated in the text. (B) Plot of the 10-kG molar susceptibilty per Ni ion vs $1/T$ for urease (●) pH 7.0. The solid line is the best fit to the data using a weighted combination of binuclear and mononuclear spin Hamiltonians and fit parameters indicated in the text; the appropriately weighted binuclear (-·-) and mononuclear (---) contributions that sum to the best fit (—) are also indicated.

recent Ni-CPA crystal structure,[9] we have remeasured the susceptibility of Ni-CPA. Our data (Figure 1B) was collected on a solution sample with 71% peptidase activity,[28] and a wider temperature range and larger magnetic field have been used than in the earlier study. We find an effective magnetic moment of 3.09 ± 0.10 μ_B for Ni-CPA. As with urease, this value is in the range expected for $\sim O_h$ coordination, in agreement with the Ni-CPA ligand field spectral data.[10] In contrast to urease, however, Ni-CPA exhibits a much smaller deviation from the Curie law behavior at low temperature.

While Ni-CA does not retain[8] the catalytic activity of the native enzyme, preparation of this derivative by stoichiometric reconstitution of apo-CA with Ni(II) leads to a well-defined protein form with the Ni(II) ion replacing the Zn(II) in the active site. Our susceptibility data (Figure 1C) for Ni-CA at pH 7.8 reveal an effective magnetic moment of 2.93 ± 0.07 μ_B that is indicative of $\sim O_h$ coordination for Ni(II) in carbonic anhydrase and consistent with the Ni-CA ligand field spectral data.[11] The deviation from the Curie law behavior at low temperature is somewhat larger in magnitude than that observed for Ni-CPA but significantly less than that exhibited by urease.

The 240–6 K magnetic data for the three Ni–protein samples in Figure 1 and additional 6–2 K data have been replotted in Figure 2A to show the 50-kG magnetization as a function of temperature and field from 240 to 2 K. In order to quantify the low-temperature deviations from the Curie law, these data were fit to the single-ion spin Hamiltonian

$$H = DS_z^2 + g\beta HS_i \qquad i = x, y, z \tag{1}$$

By varying the isotropic g value and D,[29] we have obtained good fits (Figure 2A, solid lines) of these data, for Ni-CPA with $g = 2.16$ and $D = 3.5$ cm^{-1} and for Ni-CA with $g = 2.10$ and $D = -8.2$ cm^{-1}; including a rhombic term, $E(S_x^2 - S_y^2)$, in this Hamiltonian and varying E did not significantly alter the good quality of these fits. However, the urease data could not be fit to this Hamiltonian, even by including the rhombic term and varying E up to the limit $D/3$. While the saturation behavior of the urease data would correspond in this model to $|D| \sim 25$ cm^{-1}, this value provides a poor fit (not shown) at higher temperatures. Further, this magnitude of the axial zero-field splitting is unreasonable for six-coordinate Ni(II), which is indicated for urease by the μ_{eff} value (vide supra) and ligand field spectral data (vide infra).

Since the fit of the urease data to a single-ion Hamiltonian was poor, we evaluated whether the deviation from the Curie law behavior was due primarily to an antiferromagnetic exchange interaction between the two Ni(II) ions. The data were fit to a Hamiltonian containing only isotropic exchange and the Zeeman interaction

$$H = -2J\mathbf{S}_1\cdot\mathbf{S}_2 + g\beta HS_i \qquad i = x, y, z \tag{2}$$

However, the best fit (not shown) achieved by varying g and J was comparably poor to that with the single-ion Hamiltonian.

To include both single-ion and binuclear contributions in analyzing the urease magnetic data, we have collected 10-kG magnetic susceptibility data from 200 to 6.5 K (Figure 2B) and employed the widely used formalism of Ginsberg et al.[30] and the Hamiltonian

$$H = -2J\mathbf{S}_1\cdot\mathbf{S}_2 + D[S_{1z}^2 + S_{2z}^2] + g\beta H(\mathbf{S}_1 + \mathbf{S}_2) \tag{3}$$

The interdimer exchange term in Ginsberg's original Hamiltonian has been neglected as the urease Ni(II) sites are magnetically insulated by the protein. D and g are assumed to be the same for both Ni(II) ions since the ligand field absorption data (vide infra) indicate that the urease Ni(II) ions have similar coordination sites. The lower field data are required for this analysis primarily because the Zeeman interaction is treated as a perturbation, which is valid only when the field-dependent Zeeman term is small relative to J and D and the field-independent Van Vleck equation[14a] is used to calculate the powder susceptibility. However, a reasonable fit of this data cannot be found with this binuclear Ni model by varying the exchange and axial zero-field splitting over a wide range of magnitude and considering all possible combinations of the sign of J and D; g was constrained to values consistent with the urease effective magnetic moment.

Only by inclusion of a small magnetic contribution of mononuclear Ni(II) is a satisfactory fit (Figure 2B, solid line) achieved by using the relationship

$$\chi_{m(measd)} = (1 - \alpha)\chi_{m(dimer)} + \alpha\chi_{m(monomer)} \tag{4}$$

and the binuclear (eq 3) and mononuclear (eq 1) Hamiltonians with the Van Vleck equation for the powder susceptibility. The best fit, achieved by varying J, D, and α, indicates a 78% binuclear contribution with $g = 2.2$, $J = -6.3$ cm^{-1}, and $D = -6.9$ cm^{-1} and a 22% mononuclear contribution with $g = 2.2$ and $D = -6.9$ cm^{-1}. Also indicated in Figure 2B are the appropriately weighted bi-

(27) Rosenberg, R. C.; Root, C. A.; Wang, R.-H.; Cerdonio, M.; Gray, H. B. *Proc. Natl. Acad. Sci. U.S.A.* **1973**, *70*, 161–163.

(28) At least 60% of this activity can be associated with Ni-CPA based on the 0.44 mol equiv of Ni; the remaining activity is due to residual Zn-CPA.

(29) We report the sign of D used to obtain the indicated fits; however, in fitting this data, we are not able to distinguish positive and negative D values of comparable magnitude. The sign of D can be experimentally obtained through single-crystal magnetic measurements or detailed ligand field analysis.

(30) Ginsberg, A. P.; Martin, R. L.; Brookes, R. W.; Sherwood, R. C. *Inorg. Chem.* **1972**, *11*, 2884–2889.

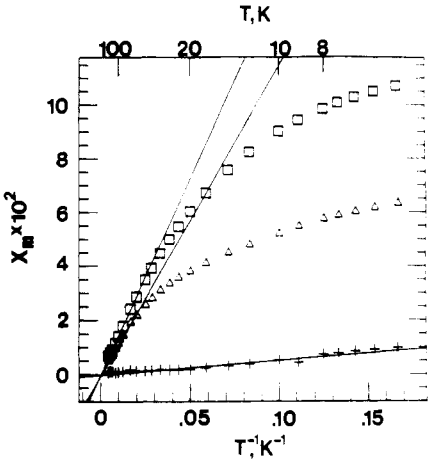

Figure 3. Plot of the 50-kG molar susceptibility per Ni ion vs $1/T$ for urease (△), urease with 10 mM acetohydroxamic acid (□), and urease with 15 mM 2-mercaptoethanol (+) (all samples pH 7.0). Solid lines are best linear fits for the $T \geq 60$ K urease data, the $T \geq 50$ K AHA-urease data, and all of the 2-ME-urease data.

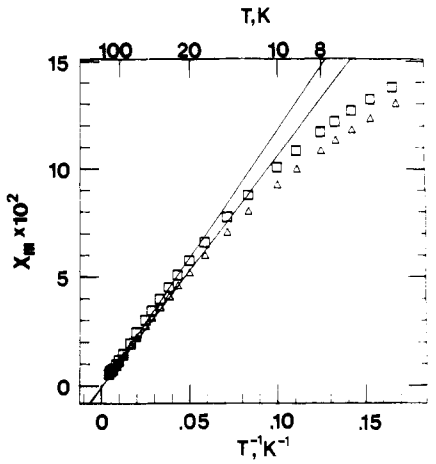

Figure 4. Plot of the 50-kG molar susceptibility per Ni ion vs $1/T$ for Ni-CA (△) and Ni-CA with 15 mM 2-mercaptoethanol (□) (both samples pH ~7.8). Solid lines are best linear fits for the $T \geq 30$ K data of each sample.

nuclear and mononuclear magnetic contributions, which sum to the observed 10-kG susceptibility. To constrain the number of fit parameters, g was fixed at 2.2 and the same g and D values were used for both the binuclear and mononuclear contributions. As before, the ligand field data (vide infra) indicate that the urease Ni(II) ions are in similar coordination environments, suggesting that the D value of the monomeric component is not significantly different than that of the dominant binuclear Ni(II) ions.

In achieving this good fit, we have found that the dominant terms are J and α, the percentage of mononuclear Ni(II). To obtain additional confidence in the low-field fit values, we have gone back and fit the 50-kG urease magnetization data to a binuclear Ni(II) contribution with isotropic exchange only (eq 2) and a mononuclear Ni(II) contribution represented by an $S = 1$ Brillouin function,[14] both with g fixed at 2.2. Figure 2A shows that a quite good fit of the urease data can be obtained with the parameters $J = -5.5$ cm^{-1} and $\alpha = 0.28$. The small discrepancy between these values and those obtained from the fit of the 10-kG data likely results from the neglect of single-ion axial zero-field splitting in this analysis.

Competitive inhibitors are important probes for substrate–enzyme interaction, and we have obtained magnetic susceptibility data for two competitive-inhibitor-bound forms of urease. Figure 3 shows the temperature-dependent χ_m vs $1/T$ data for native urease, urease in the presence of 10 mM acetohydroxamic acid (AHA), and urease in the presence of 15 mM 2-mercaptoethanol (2-ME).

Acetohydroxamic acid is a very potent inhibitor of urease ($K_i = 4$ μM at 25 °C)[15] and other metalloenzymes; this behavior likely relates to the high binding affinity of this potentially chelating ligand for metal ions. When AHA is added to native urease, the magnetic susceptibility data (Figure 3) show that there is a significant increase in the average effective magnetic moment per Ni(II) ion to 3.39 ± 0.12 μ_B and a smaller deviation from the Curie law behavior at low temperature.

2-Mercaptoethanol is a less potent inhibitor of urease ($K_i = 0.7$ mM at 25 °C)[31] than AHA. However, the appearance of new absorption and CD bands[3,4,32] in the near-UV region upon addition of 2-ME to urease suggests that it binds directly to the Ni(II) ion(s); the presence of Ni–S ligation upon 2-ME binding has been confirmed by recent X-ray absorption data.[6] The magnetic susceptibility data (Figure 3) for 2-ME-bound urease indicates that this thiolate competitive inhibitor causes a major change in the Ni(II) ground state, reversibly resulting in a *diamagnetic* Ni(II) form for 78%[33] of the urease; this phenomenon is also observed for other thiolate inhibitors.[4] The susceptibility of this protein form is observed to be linear to the highest temperature measurement (240 K), indicating negligible population of higher energy paramagnetic states.

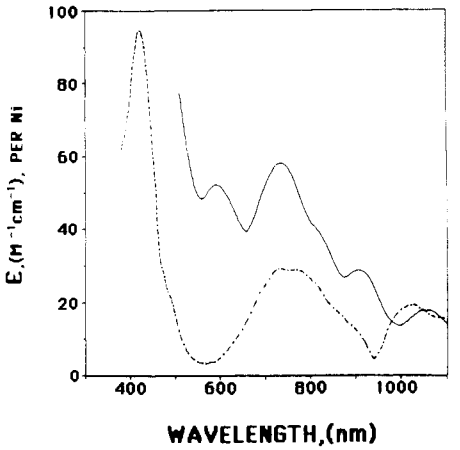

Figure 5. Visible and near-IR absorption data for urease (–·–) and urease in the presence of 20 mM 2-ME (—) (both samples pH 7.0).

In order to evaluate the generality of this dramatic effect of thiolate binding on the urease Ni(II) ground state, we have obtained susceptibility data for the 2-ME-bound form of Ni-CA. A new absorption band at 380 nm ($\epsilon \approx 500$ M^{-1} cm^{-1}) is observed[34] upon addition of 2-ME to Ni-CA, suggesting direct thiolate coordination to the Ni(II) ion as found for urease.[6] However, as shown in Figure 4, the bound thiolate has very little effect on the ground state of the Ni(II) ion in carbonic anhydrase; the effective magnetic moment is only raised slightly to 3.09 ± 0.08 μ_B, and the low-temperature deviation from the Curie law behavior (zero-field-splitting) is not significantly altered. This suggests a unique interaction between thiolate inhibitors and the urease Ni(II) ion(s), leading to the observed diamagnetism.

To further evaluate the effect of thiolate binding on the ground state of the urease Ni(II) ions, we have obtained ligand field absorption spectra of native and 2-ME-bound urease (Figure 5). For native urease, three distinct absorption bands are observed at 425 ($\epsilon < 95$ M^{-1} cm^{-1}; this value contains a contribution from

(31) Dixon, N. E.; Blakeley, R. L.; Zerner, B. *Can. J. Biochem.* **1980**, *58*, 481–488.
(32) Nagarajan, N.; Fishbein, W. N. *Fed. Proc., Fed. Am. Soc. Exp. Biol.* **1977**, *36*, 700.
(33) The observed residual magnetic moment (0.66 ± 0.04 μ_B) does not have the correct temperature dependence to attribute it to dissolved oxygen or to population of the paramagnetic states of an exchange-coupled Ni(II) site; a similar residual moment is found with D_2O buffer and a quartz bucket ruling out magnetic noise (ref 26). This weak susceptibility data does, however, appear to have the temperature profile of zero-field-split Ni(II) and quantitatively correlates with 22% of the urease Ni(II) ions.
(34) Goldman, J. D.; Wilcox, D. E. To be submitted for publication.

the tail of the 280-nm protein absorption), ~750 (ϵ = 30 M^{-1} cm^{-1}), and 1020 nm (ϵ = 20 M^{-1} cm^{-1}); the middle band is broad and apparently split. These data are quantitatively different than that previously reported[3] for native urease. While a complete ligand field analysis of the urease Ni(II) ions will require variable-temperature absorption, CD, and MCD data, the d–d absorption bands of native urease strongly suggest that all the Ni(II) ions in urease have similar ~O_h coordination sites in agreement with the magnetic data. Upon addition of 20 mM 2-ME, changes are observed in the Ni(II) ligand field bands. New features are found at 590 and 910 nm, the broad split band at ~750 nm sharpens and shifts to 730 nm, the 1020-nm band shifts to 1060 nm, and the 425-nm band appears to increase in intensity and shift to 420 nm (not shown; but see ref 3). This absorption spectrum is remarkably similar to that previously reported[3] for native urease but obtained in the presence of 1 mM 2-ME. While clearly there are some changes in the Ni(II) ligand field spectrum upon 2-ME binding, most of the increased intensity, especially in the 425-nm band, is due to the tail of the intense higher energy thiolate-to-Ni(II) charge-transfer transitions.[3,4]

Discussion

Comparison of the magnetic moments of the Ni(II) ions in urease, Ni-CPA, and Ni-CA to those of structurally defined Ni(II) complexes indicates that all three proteins have six-coordinate Ni(II) sites in agreement with ligand field spectral data. We have analyzed the magnetization data for the three Ni proteins to further determine their ground-state electronic properties and structural information about their Ni sites. The discussion of these results follows, beginning with the two mononuclear Ni(II) enzymes, which provide an important basis for comparison to urease.

Ni-CPA. In spite of retaining significant peptidase and esterase activity, the Ni-substituted form of carboxypeptidase has been the subject of only limited characterization. The Ni(II) ligand field absorption spectrum indicated[10] ~O_h coordination, while crystallography showed[9] the Ni ion to have a square-pyramidal geometry; further, the Ni(II) magnetic moment was reported[27] to be lower than the spin-only value. However, it is known[35] that the catalytic activity of crystallized carboxypeptidase is quite variable, and the crystallographic study of Ni-CPA was performed on crystals of unreported catalytic activity; this is also true of the desiccated Ni-CPA sample used in the earlier magnetic susceptibility study. The ligand field absorption spectra, though, were obtained on samples with 70–90% peptidase activity relative to native carboxypeptidase. The ~O_h Ni(II) coordination indicated by our magnetic susceptibility measurement (μ_{eff} = 3.09 ± 0.10 μ_B) on Ni-CPA with 71% peptidase activity[28] is thus consistent with the ~O_h Ni(II) coordination indicated by the ligand field transitions in catalytically active Ni-CPA. Fitting the Ni-CPA magnetization data (Figure 2A) indicates an axial zero-field splitting (D = 3.5 cm^{-1}) of the $^3A_2$ ground state that is consistent with a somewhat distorted six-coordinate geometry for Ni(II) in the CPA active site. A larger effective magnetic moment, a larger axial zero-field splitting, and possibly rhombic splitting might be expected if the crystallographically determined distorted-square-pyramidal Ni(II) was found in high-activity solution Ni-CPA. However, if this five-coordinate form of Ni-CPA has a $^1A_1$ ground state (diamagnetic), then a small percentage of this form in the sample previously studied by magnetic susceptibility could explain the reported[27] low magnetic moment of Ni-CPA. Further study of crystalline and solution Ni-CPA is warranted to address these electronic and structural questions.

Ni-CA. The crystal structure of native carbonic anhydrase shows[36] the Zn(II) ion bound to three histidines and a water or hydroxide. While no structural information is currently available on Ni-CA, the energies and intensities of the Ni(II) ligand field transitions have been interpreted[11] to suggest a six-coordinate geometry near neutral pH. The effective magnetic moment we measure (μ_{eff} = 2.93 ± 0.07 μ_B) at pH ~7.8 is typical for ~O_h Ni(II) and consistent with the ligand field analysis of Ni-CA. The fit of the Ni-CA magnetization data (Figure 2A) indicates that the low-temperature deviation from the Curie law corresponds to axial zero-field splitting (D = −8.2 cm^{-1}) of a six-coordinate Ni(II) site somewhat more distorted than that of Ni-CPA.

The intensities of the Ni(II) ligand field bands of Ni-CA show a strong pH dependence that has been interpreted[11] as indicating a change in the Ni(II) coordination at high pH. Our magnetic data were obtained at a pH value closer to the low pH side of these spectral changes where ~O_h Ni(II) coordination has been suggested; however, the axial zero-field splitting we measure at pH ~7.8 may reflect contributions from a higher pH form with a different Ni(II) coordination. Additional characterization of the Ni-CA magnetic properties will be required to further elucidate the pH-dependent Ni(II) electronic and structural properties that may relate to the pH dependence of carbonic anhydrase catalytic activity.

Urease: Native Susceptibility. New information about the electronic and geometric properties of the Ni ions in urease are required for a better understanding of the enzyme active site and the Ni(II) mechanistic role. This study has shown that both of the Ni(II) ions in the urease subunit are paramagnetic (μ_{eff}/Ni ion = 3.04 ± 0.10 μ_B) with ~O_h coordination and $^3A_2$ ground states. This interpretation is consistent with the three weak ligand field transitions observed in the absorption spectrum (Figure 5) of native urease.

In contrast to Ni-CA and Ni-CPA, however, we are unable to fit the urease 50-kG magnetization data (Figure 2A) to a single-ion spin Hamiltonian. While the saturated magnetization at the lowest temperature would infer a single-ion axial zero-field splitting on the order of 25 cm^{-1}, this gives an unacceptable fit to the rest of the magnetization data, even including rhombic splitting, and is an unreasonable value for six-coordinate Ni(II). The dramatic low-temperature deviation from the Curie law observed for urease therefore indicates additional perturbation(s) of the Ni(II) ground state. On the basis of the similarity of the effective magnetic moments of Ni-CPA, Ni-CA, and urease and the similarity of the ligand field spectra of Ni-CPA[10] and urease (Figure 5), yet the dramatically different low-temperature magnetization behavior of urease compared to the single-ion magnetization data for Ni-CPA and Ni-CA, we are led to conclude that there is a magnetic interaction between the two paramagnetic Ni(II) ions in the urease subunit.

However, attempts to fit the urease susceptibility data to a Hamiltonian including isotropic exchange interaction and to the Ginsberg model, which includes both isotropic exchange and single-ion axial zero-field splitting, also proved to be unsuccessful. The poor quality of the latter fit was unexpected since this model has worked quite well for numerous O_h and tetragonal Ni(II) dimers with either ferromagnetic or antiferromagnetic interaction.[37-40] It is possible to estimate from the urease susceptibility and absorption data the magnitude of J and D, respectively. A maximum (Neel point) in the plot of χ vs T will indicate the magnitude of antiferromagnetic coupling, while a positive anomoly in the μ_{eff} vs T plot indicates ferromagnetic exchange. Unfortunately neither feature is observed in the urease data (plots not shown), indicating that J is small (on the order of a few wavenumbers) or that these features are masked by other effects. The ligand field absorption data provides an estimate of the urease Ni(II) zero-field splitting; structural distortions from O_h symmetry lead to a splitting of the lowest energy $^3T_2 \leftarrow {}^3A_2$ ligand field band which, through spin–orbit coupling, ultimately results in the zero-field splitting of the ground state. Our urease absorption data (Figure 5) appear to indicate that any splitting of this feature at 1020 nm is unresolvable,[45] and the $|D|$ value is not expected

(35) Spilburg, C. A.; Bethune, J. L.; Vallee, B. L. *Biochemistry* **1977**, *16*, 1142–1150.
(36) Kannan, K. K.; Nostrand, B.; Fridborg, K.; Lovgren, S.; Ohlsson, A.; Petef, M. *Proc. Natl. Acad. Sci. U.S.A.* **1975**, *72*, 51–55.
(37) Laskowski, E. J.; Felthouse, T. R.; Hendrickson, D. N.; Long, G. L. *Inorg. Chem.* **1976**, *15*, 2908–2911.
(38) Duggan, D. M.; Hendrickson, D. N. *Inorg. Chem.* **1973**, *12*, 2422–2431.
(39) Duggan, D. M.; Hendrickson, D. N. *Inorg. Chem.* **1974**, *13*, 2929–2940.
(40) Landee, C. P.; Willett, R. D. *Inorg. Chem.* **1981**, *20*, 2521–2525.

to be larger than ~ 10 cm^{-1}. Further, the absorption data also suggest that there is no major difference in the coordination of the Ni(II) ions. Thus, the Ni(II) ions in urease appear to be in similar $\sim O_h$ coordination sites, there appears to be only weak Ni(II)–Ni(II) magnetic interaction, and the formalism of Ginsberg et al.[30] should be appropriate.

Certain approximations are built in to the Ginsberg model for fitting binuclear Ni(II) magnetic susceptibility. First, at 10 kG the magnetic field may be too large to treat the Zeeman interaction (~ 1 cm^{-1} at this field) as a perturbation if the exchange interaction and zero-field splitting are of comparable magnitude; however, magnetic data for other Ni(II) dimers at similar fields have been reasonably fit with J and D parameters on this order of magnitude. Second, although the urease data at 10 kG may not be field independent, which this model requires, the errors introduced should be small at this magnetic field. Third, anisotropic or antisymmetric exchange will also be small[41] for the case of the orbitally nondegenerate $^3A_{2g}$ ground state of O_h Ni(II) and any effective symmetries derived from O_h in urease. Further, the urease ligand field data does not distinguish differences between the $\sim O_h$ coordination environments of each Ni(II) ion. Therefore the Ginsberg binuclear model should be appropriate for fitting the urease 10-kG magnetic susceptibility.

The shape of the 10-kG urease susceptibility data, however, does suggest an origin for the poor fit. The curvature of the susceptibility data in the temperature range 60 K > T > 30 K is most sensitive to the magnitude of J (the single Ni(II) ions in Ni-CPA and Ni-CA exhibit linear Curie law behavior in this temperature range), yet the value required to fit this region leads to a Neel point and diminished susceptibility at low temperature. The urease data, however, continue to increase at low temperature, and no magnitude of D provides a reasonable fit. Thus it appears that another paramagnetic component contributes to the observed susceptibility, and we can achieve a good fit of the data (Figure 2B) if 22% of the paramagnetism is attributed to mononuclear Ni(II). Figure 2B shows both the appropriately weighted binuclear and mononuclear contributions; a Neel point is observed for the binuclear Ni(II) urease active site susceptibility data, but this is masked by the susceptibility of the minor mononuclear Ni(II) component. We gain additional confidence in this interpretation based on our ability to fit the urease 50-kG data to a Hamiltonian including contributions from an isotropically exchange coupled Ni(II) dimer and a mononuclear Ni(II) component (Figure 2A).

Inclusion of a mononuclear component is commonly necessary when fitting the magnetic data of synthetic binuclear small molecule complexes but is not expected to be necessary for high-purity and high-activity urease. However, the magnetic data with 2-ME suggests that there is a $\sim$20% subset[33] of urease Ni(II) ions that behave differently with respect to this thiolate competitive inhibitor. While further studies will be necessary to determine if the same sites are responsible for both effects, we feel this similar behavior lends support for our fit which includes a $\sim$20% subset of urease sites that exhibit magnetic susceptibility of noninteracting Ni(II) ions. Future studies will be aimed at determining the origin of this heterogeneous subset of urease sites.

The parameters required to fit the native urease magnetic susceptibility data, g = 2.2, J = −6.3 cm^{-1}, and D = −6.9 cm^{-1} indicate for the first time that the active site consists of a weakly antiferromagnetic exchange-coupled pair of $\sim O_h$ Ni(II) ions. The strength of this interaction is larger than would be found with a purely dipolar interaction between two S = 1 ions at any reasonable separation and thus requires a bridging ligand superexchange pathway. The magnitude of the J value does not yet appear to limit the possible bridge candidates or indicate whether a protein or exchangeable ligand is involved. Further chemical and spectroscopic studies will be required to refine this developing model of the binuclear Ni(II) urease active site.

Urease: Inhibitor-Bound Susceptibility. Binding of the competitive inhibitor acetohydroxamic acid leads to a significant increase in the urease Ni(II) magnetic moment. Since the urease Ni(II) ligand set contains only N and O donor ligands[5,6] and AHA binding should not significantly change the type of ligand atoms, the observed increase in the Ni(II) moment likely indicates a change in the coordination number and/or geometry of the required Ni(II) ion(s) upon binding of this competitive inhibitor. Further, this perturbation affects the magnitude of the weak exchange interaction between the Ni(II) ions as evidenced by the diminuation of the low-temperature deviation from the Curie law. The bulk magnetic susceptibility data, however, are not capable of indicating if this change is taking place at one or both of the urease Ni(II) ions; a detailed analysis of the accompanying ligand field spectral changes will be required to address this question.

The reversible loss of paramagnetism upon thiolate binding to urease could be due to a $^1A_1$ ground state of each Ni(II) resulting from a tetragonal low-spin Ni(II) ligand field upon thiol ligation. Typically, an intense orbitally allowed d–d transition (square pyramid C_{4v}, $^1E \leftarrow {}^1A_1$; trigonal bipyramid D_{3h}, $^1E' \leftarrow {}^1A_1'$; distorted square planar D_{2d}, $^1E \leftarrow {}^1A_1$) is associated[42] with four- and five-coordinate low-spin Ni(II). While there are differences (Figure 5) between the ligand field absorption spectra of native urease and 2-ME-bound urease, the intense orbitally allowed ligand field transition(s) expected for low-spin Ni(II) are not observed. Further, recent Ni X-ray absorption results[6] indicate there is no major change in the urease Ni(II) site symmetry upon 2-ME binding and further argue against a change to a low-spin ligand field.

Alternatively, the diamagnetic thiolate complex could result from strong antiferromagnetic interaction between the two S = 1 ions upon thiolate binding. This could be an increase in the intrinsic antiferromagnetic exchange or a new interaction mediated by a bridging thiolate. Since the magnetic susceptibility data from 6 to 240 K show no deviation from the Curie law behavior of the residual moment, an antiferromagnetic coupling with a large singlet–triplet splitting (>200 cm^{-1}) would be required for negligible population of the paramagnetic triplet state at the higher temperatures. While there are examples[43,44] of diamagnetic μ-thiolato–Ni(II) dimers, the diamagnetism in each case appears to be due to a $^1A_1$ ground state of each Ni(II) resulting from square-planar coordination and not due to thiolate-mediated exchange coupling. The change in the urease Ni(II) ground state upon thiolate inhibitor binding, however, appears to be associated with a strong antiferromagnetic interaction between the Ni(II) ions; support for this assignment, though, now requires appropriate model complexes. However, of possible relevance to the Ni(II) mechanistic role in urease, we note that a bridging competitive inhibitor may require a bridging binding mode for the substrate urea.

The residual magnetic moment found with 2-ME corresponds to $\sim$20% of the urease Ni(II) ions and may be associated with active sites inaccessible to the thiolate or due to a subset of sites where 2-ME binds differently. In fact, the latter explanation is consistent with the result (vide supra) that under these conditions $\sim$20% of the urease active sites show no magnetic interaction between the Ni(II) ions and are likely to bind 2-ME differently, possibly in a nonbridging geometry, than the dominant 80% of the sites. Further study will be required to determine the origin and properties of this subset of urease active sites that exhibit different chemical and magnetic properties.

In summary, the major difference between the magnetic properties of the urease Ni(II) ions and those of Ni-CPA and Ni-CA is the significantly larger deviation from the Curie law behavior observed for urease at low temperature. For Ni-CPA and Ni-CA, this deviation is due to axial zero-field splitting of the $^3A_2$ ground state and reflects the deviations from O_h symmetry

(41) Ginsberg, A. P. *Inorg. Chim. Acta Rev.* **1971**, *5*, 45–68.
(42) Lever, A. B. P. *Inorganic Electronic Spectroscopy*, 2nd ed.; Elsevier: Amsterdam, 1984.
(43) Snyder, B. S.; Rao, C. P.; Dorfman, J. R.; Holm, R. H. *Aust. J. Chem.* **1986**, *39*, 963–974 and references therein.
(44) McKenzie, C. J.; Robson, R. *Inorg. Chem.* **1987**, *26*, 3615–3621.
(45) In addition to the 1020-nm band, features at $\lambda > 1100$ nm may be associated with splitting of this transition; however, it is unreasonable for six-coordinate Ni(II) to have $|D| \gtrsim 10$ cm^{-1}.

of the Ni(II) ions in these protein active sites. By comparison, however, the urease magnetic data indicate additional perturbation of the Ni(II) ground state due to a weak exchange interaction between the two Ni(II) ions in the catalytically active subunit. Binding of thiolate inhibitors appears to result in a large antiferromagnetic interaction between the urease Ni(II) ions and suggests the possibility of bridging coordination of substrates. Additional studies of the magnetic and spectroscopic properties of this enzyme will further evaluate the Ni–Ni interaction to elucidate structural, electronic, and catalytic properties of the urease binuclear nickel active site.

Acknowledgment. We thank Richard Frankel for use of the SQUID magnetometer facility at the Francis Bitter National Magnet Laboratory, MIT, and Christopher Reed and Carol Koch for assistance with the USC SQUID magnetometer purchased with funding from the NSF. We thank Edmund Day for a preprint of ref 26 and useful discussions. We also thank Kevos Spartalian, Robert Ditchfield, and Robert Cantor for helpful discussions and Norma Leonida and John Goldman for technical assistance. We are grateful for a Bristol-Myers Co. Grant from the Research Corp. and for USDA Competitive Research Grant No. 87-CRCR-1-2485, which supported this research.

Contribution from the Department of Chemistry,
University of Texas, Austin, Texas 78712

Binding of Pyridine and Benzimidazole to a Cadmium "Expanded Porphyrin": Solution and X-ray Structural Studies

Jonathan L. Sessler,* Toshiaki Murai, and Vincent Lynch

Received October 5, 1988

The characterization by X-ray diffraction analysis of a six-coordinate pentagonal-pyramidal cadmium(II) cationic complex **4b** derived from a novel aromatic 22-π-electron pentadentate "expanded porphyrin" ligand (**2**) is described. $Cd(C_{32}H_{34}N_5)(C_7H_6N_2)NO_3 \cdot CHCl_3$ crystallizes in the triclinic space group $P\bar{1}$ (No. 2) in a cell of dimensions a = 11.276 (4) Å, b = 12.845 (3) Å, c = 14.913 (4) Å, α = 84.82 (2)°, β = 69.57 (2)°, γ = 85.84 (2)°, and V = 2014 (1) Å^3 with Z = 2. The structure was solved by the heavy-atom method and refined by full-matrix least squares in blocks of 253 and 287 parameters. The final R = 0.0781 and R_w = 0.114 from 3294 reflections with $F_o > 6(\sigma(F_o))$. The X-ray structure reveals the five central donor atoms of the macrocycle to be coordinated to the cadmium(II) cation, which in turn lies 0.334 (2) Å above the mean plane of the macrocycle and is further ligated by an apical benzimidazole ligand. As is true in the corresponding pentagonal-bipyramidal bis(pyridine) adduct **5a**, the X-ray structure of cation **4b** indicates the macrocyclic ligand to be nearly planar (maximum deviation 0.154 (13) Å for C15) with the five donor nitrogen atoms defining a near-circular cavity with a center-to-nitrogen radius of $\simeq$2.42 Å. The crystals of **4b**(NO_3) used for the X-ray diffraction analysis were isolated from an inhomogeneous mixture of crystalline and noncrystalline material obtained following treatment of the sp^3 form of the ligand (**1**) with $Cd(NO_3)_2 \cdot 4H_2O$ and subsequent purification on Sephadex. The proton NMR spectrum in $CDCl_3$ of this bulk material is essentially identical with that of the pure five-coordinate complex **3** prepared independently but showed the presence of a broad feature at ca. 6.4 ppm and two sharper peaks at 6.81 and 7.27 ppm ascribable to the bound benzimidazole ligand. These diagnostic ligand features are reproduced upon titrating the pure five-coordinate complex **3** with roughly $^3/_5$ equiv of benzimidazole. This finding suggests that the bulk material from which crystals of **4b**(NO_3) were isolated consists of a mixture of crystalline and noncrystalline six- and five-coordinate species and supports the hypothesis that the bound benzimidazole found in cation **4b** is derived from degradative side reactions associated with the metal insertion and accompanying ligand oxidation. From these titrations the values for the sequential formation constants (K_1 and K_2) for the binding of the first and second equivalents of benzimidazole to the five-coordinate cationic complex **3** were determined to be 1.8 × 10^4 and 13 M^{-1}, respectively. For the complexation of pyridine to **3**(NO_3), K_1 and K_1K_2 values of 1.6 M^{-1} and 315 M^{-2}, respectively, were determined from similar ^{1}H NMR titrations. These results indicate that in benzimidazole-containing chloroform solutions an extended concentration range exists wherein the *pentagonal-pyramidal* complex **4b** is the primary cadmium-containing species, whereas in the presence of pyridine it is either the unligated complex **3** or the coordinatively saturated *pentagonal-bipyramidal* species **5a** that will dominate in solution.

Although the porphyrins and related tetrapyrrolic compounds remain among the most widely studied of all known macrocycles,[1] relatively little effort has been devoted to the development of larger conjugated pyrrole-containing systems.[2-12] Large, or "expanded", porphyrin-like systems, however, are of interest for several reasons: They could serve as possible aromatic analogues of the better

(1) *The Porphyrins*; Dolphin, D., Ed.; Academic Press: New York, 1978–1979; Vol. I–VII.
(2) (a) Day, V. W.; Marks, T. J.; Wachter, W. A. *J. Am. Chem. Soc.* **1975**, *97*, 4519–4527. (b) Marks, T. J.; Stojakovic, D. R. *J. Am. Chem. Soc.* **1978**, *100*, 1695–1705. (c) Cuellar, E. A.; Marks, T. J. *Inorg. Chem.* **1981**, *20*, 3766–3770.
(3) Bauer, V. J.; Clive, D. R.; Dolphin, D.; Paine, J. B., III; Harris, F. L.; King, M. M.; Loder, J.; Wang, S.-W. C.; Woodward, R. B. *J. Am. Chem. Soc.* **1983**, *105*, 6429–6436. To date only tetracoordinated metal complexes have been prepared from these potentially pentadentate ligands.
(4) Broadhurst, M. J.; Grigg, R.; Johnson, A. W. *J. Chem. Soc., Perkin Trans. 1* **1972**, *2111*–2116.
(5) Broadhurst, M. J.; Grigg, R.; Johnson, A. W. *J. Chem. Soc. D* **1969**, 23–24. Broadhurst, M. J.; Grigg, R.; Johnson, A. W. *J. Chem. Soc. D* **1969**, 1480–1482. Broadhurst, M. J.; Grigg, R.; Johnson, A. W. *J. Chem. Soc. D* **1970**, 807–809.
(6) (a) Berger, R. A.; LeGoff, E. *Tetrahedron Lett.* **1978**, 4225–4228. (b) LeGoff, E.; Weaver, O. G. *J. Org. Chem.* **1987**, *52*, 710–711.
(7) (a) Rexhausen, H.; Gossauer, A. *J. Chem. Soc., Chem. Commun.* **1983**, 275. (b) Gossauer, A. *Bull. Soc. Chim. Belg.* **1983**, *92*, 793–795.
(8) (a) Gosmann, M.; Franck, B. *Angew. Chem.* **1986**, *98*, 1107–1108; *Angew. Chem., Int. Ed. Engl.* **1986**, *25*, 1100–1101. (b) Knübel, G.; Franck, B. *Angew. Chem.* **1988**, *100*, 1203–1205; *Angew. Chem., Int. Ed. Engl.* **1988**, *27*, 1170–1172.
(9) For examples of porphyrin-like systems with *smaller* central cavities see: (a) Vogel, E.; Kocher, M.; Schmickler, H.; Lex, J. *Angew. Chem.* **1986**, *98*, 262–263; *Angew. Chem., Int. Ed. Engl.* **1986**, *25*, 257–258. (b) Vogel, E.; Balci, M.; Pramod, K.; Koch, P.; Lex. J.; Ermer, O. *Angew. Chem.* **1987**, *99*, 909–912; *Angew. Chem., Int. Ed. Engl.* **1987**, *26*, 928–931.
(10) For examples of large nonaromatic pyrrole-containing macrocycles see: (a) Acholla, F. V.; Mertes, K. B. *Tetrahedron Lett.* **1984**, 3269–3270. (b) Acholla, F. V.; Takusagawa, F.; Mertes, K. B. *J. Am. Chem. Soc.* **1985**, *107*, 6902–6908. (c) Adams, H.; Bailey, N. A.; Fenton, D. A.; Moss, S.; Rodriguez, de Barbarin, C. O.; Jones, G. *J. Chem. Soc., Dalton Trans.* **1986**, 693–699. (d) Fenton, D. E.; Moody, R. *J. Chem. Soc., Dalton Trans.* **1987**, 219–220.
(11) Sessler, J. L.; Murai, T.; Lynch, V.; Cyr, M. *J. Am. Chem. Soc.* **1988**, *110*, 5586–5588.

0020-1669/89/1328-1333$01.50/0